Heliyon 10 (2024) e36267

Contents lists available at ScienceDirect

Heliyon

journal homepage: www.cell.com/heliyon

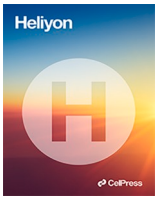

Research article

Integrated network pharmacology and metabolomics to study the potential mechanism of Jiawei Yinchenhao decoction in chronic hepatitis B

Xinyi Xu [a,1], Jin Liu [b,1], Xue Li [a,1], QuanSheng Feng [a,**], Yue Su [a,*]

[a] College of Basic Medical Sciences, Chengdu University of Traditional Chinese Medicine, Chengdu, 611137, China
[b] College of Clinical Medicine, Chengdu University of Traditional Chinese Medicine, Chengdu, 611137, China

ARTICLE INFO

Keywords:
Jiawei Yinchenhao decoction
Chronic hepatitis B
Traditional Chinese medicine
Network pharmacology
Metabolomics

ABSTRACT

Chronic hepatitis B infection (CHB) is a major risk factor for the development of hepatocellular carcinoma (HCC) globally and continues to pose a significant global health challenge. Jiawei Yinchenhao decoction (JWYCH) is a modified version of Yinchenhao decoction (YCHD), which is widely used to treat liver diseases including icteric hepatitis, cholelithiasis, and hepatic ascites. However, the effectiveness and underlying mechanism of JWYCH on CHB are still unclear. This study aimed to investigate the impact of JWYCH on CHB and explore the underlying mechanism via network pharmacology and metabolomics. C57BL/6 mice were administered rAAV-HBV1.3 via hydrodynamic injection (HDI) to establish the CHB model. The infected mice were orally administered JWYCH for 4 weeks. HBsAg, HBeAg, HBV DNA, the serum liver function index, and histopathology were detected. In addition, network pharmacology was used to investigate potential targets, whereas untargeted metabolomics analysis was employed to explore the hepatic metabolic changes in JWYCH in CHB mice and identify relevant biomarkers and metabolic pathways. JWYCH was able to reduce HBeAg levels and improve liver pathological changes in mice with CHB. Additionally, metabolomics analysis indicated that JWYCH can influence 105 metabolites, including pipecolic acid, alpha-terpinene, adenosine, and L-phenylalanine, among others. Bile acid metabolism, arachidonic acid metabolism, and retinol metabolism are suggested to be potential targets of JWYCH in CHB. In conclusion, JWYCH demonstrated a hepatoprotective effect on a mouse model of CHB, suggesting a potential alternative therapeutic strategy for CHB. The effect of JWYCH is associated mainly with regulating the metabolism of bile acid, arachidonic acid, and retinol. These differentially abundant metabolites may serve as potential biomarkers and therapeutic targets for CHB.

1. Introduction

Hepatitis B virus (HBV) is a prevalent pathogen on a global scale, and chronic hepatitis B (CHB), a global health issue, is caused by persistent HBV infection through reverse transcription replication. Approximately 254 million people suffer from chronic hepatitis B

* Corresponding author.
** Corresponding author.
E-mail addresses: fengqs118@163.com (Q. Feng), suyue@cdutcm.edu.cn (Y. Su).
[1] These authors contributed equally to this work.

https://doi.org/10.1016/j.heliyon.2024.e36267
Received 25 February 2024; Received in revised form 1 August 2024; Accepted 13 August 2024
Available online 14 August 2024

Abbreviations

AA	arachidonic acid
ALT	alanine aminotransferase
ANIT	Alpha-naphthalene isothiocyanate
AST	aspartate aminotransferase
BA	Bile acid
CHB	chronic hepatitis B
HBV-DNA	hepatitis B virus DNA
HBeAg	HBV e antigen
HBsAg	HBV surface antigen
HBx	hepatitis B virus X protein
HDI	hydrodynamic injection
JWYCH	Jiawei Yinchenhao decoction
OPLS-DA	orthogonal partial least squares discriminant analysis
PCA	principal component analysis
rAAV-HBV1.3	recombinant adeno-associated virus carrying a 1.3-fold longer HBV genome
RA	retinoic acid
TCM	Traditional Chinese medicine
UHPLC-MS	ultrahigh-performance liquid chromatography-tandem mass spectrometry
YCHD	Yinchenhao decoction

virus infection [1], which is a leading cause of liver cirrhosis (LC) and hepatocellular carcinoma (HCC). Furthermore, HBV-related diseases lead to more over 1 million fatalities per year [2]. The functional cure is characterized by the loss of HBsAg, and the seroconversion of HBsAg is considered the desired treatment endpoint [2]. Although nucleos(t)ide analogues (NAs) and pegylated interferon α (IFNα) have been approved as therapeutic drugs, the cure rate remains below 10 % [3].

Jiawei Yinchenhao decoction (JWYCH) is composed of *Artemisia capillaris* Thunb. (Yinchen), *Rheum palmatum* L. (Dahuang), *Gardenia jasminoides* J.Ellis (Zhizi), and *Atractylodes macrocephala* Koidz. (Baizhu). Decoction refers specifically to a medicinal preparation made by boiling plant materials in water for an extended period. The decoction is a modified version of the Yinchenhao decoction (YCHD) from the classic Traditional Chinese Medicine (TCM) book "*Synopsis of the Golden Chamber*" by Zhang Zhongjing, in which the decoction was initially used to treat damp-heat jaundice. The use of baizhu is inspired by the TCM principle of "treating the liver by nourishing the spleen." Baizhu has been reported to reduce inflammation, regulate lipid levels, and demonstrate antibacterial and antiviral activity [4]. Prescriptions containing baizhu are often used for NAFLD [5,6]. Yinchen, Dahuang, and Zhizi have been found to exhibit hepatoprotective effects, facilitate liver repair, counteract steatosis, possess anti-inflammatory and antiviral properties, and even inhibit liver fibrosis. They can treat various liver-related diseases, including jaundice and viral hepatitis [7–9]. Nevertheless, the therapeutic mechanism of JWYCH in CHB remains uncertain.

The host range of HBV is limited; an appropriate animal model would facilitate the investigation of the HBV life cycle, new agent development, and the evaluation of immunotherapeutic strategies [10,11]. Hence, in this research, an AAV-HBV transduction mouse model was employed. Metabolomics examines the comprehensive alterations of small molecules within the metabolome. It can identify biomarkers indicative of disease pathways, showing promise in the field of precision medicine [12,13].

In this study, a mouse model of CHB was generated via the use of AAV-HBV, a high-fat diet, and ANIT. This study aimed to clarify the changes in the metabolites of JWYCH in a mouse model of CHB and investigate the modulatory effects of JWYCH on metabolites and potential pathways. This research holds potential for the therapeutic application of JWYCH in the treatment of CHB.

2. Materials and methods

2.1. Materials and reagents

The herbs capillary artemisia (batch no. 230501), *Rheum officinale* (batch no. 220801), and gardenia (batch no. 230501) were obtained from Sichuan Guoqiang Pharmaceutical Co., Ltd. (Sichuan, China). *Atractylodes macrocephala* (batch no. CO38230301) was purchased from Chengdu Xinfuyuan Pharmaceutical Co., Ltd. (Sichuan, China).

rAAV-HBV1.3 was obtained from PackGene Biotech (Guangzhou, China). A high-fat diet (TP23400) was purchased from Trophic Tech Co., Ltd. (Nantong, China). ANIT was obtained from Rhawn Co., Ltd. (Shanghai, China).

2.2. Preparation and UHPLC-MS/MS analysis of JWYCH

JWYCH comprises four herbs, including capillary artemisia (18 g), gardenia (12 g), *Rheum officinale* (6 g), and *Atractylodes macrocephala* (15 g). The herbs were soaked in water (1:10, w/v) for 1 h and boiled for 30 min twice. The extracts from both filtrates were mixed, and then the crude drug was diluted to a dosage of 20 mg/mL.

The analysis was conducted using the Thermo Fisher Ultimate 3000 and Q Extractive instruments, which employ an ultrahigh-performance liquid chromatography (UHPLC) AQ-C18 chromatographic column (150 mm × 2.1 mm, 1.8 μm) (Welch, Shanghai, China). The flow rate was 0.35 mL/min, and the sample injection volume was 5 μL, with a column temperature of 35 °C. The mobile phases consisted of 0.1 % formic acid in water (A) and 0.1 % acetonitrile (B). The gradient elution procedure was as follows: 0–12 min, 3–15 % B; 12–15 min, 15–18 % B; 15–18 min, 18–20 % B; 18–28 min, 20–40 % B; 28–45 min, 40–90 % B. The MS methods were as follows: spray voltage (+): 3.5 kV; spray voltage (−): 2.5 kV; capillary temperature: 350 °C; sheath gas: 40 arb; and auxiliary gas: 15 arb. The mass range for the span mode was set from *m/z* 100–1500.

2.3. Network pharmacology analysis and molecular docking

The herbs *Artemisia capillaris* Thunb., *Rheum palmatum* L., *Gardenia jasminoides* Ellis, and *Atractylodes macrocephala* Koidz. were imported into the TCMSP (https://tcmsp-e.com/tcmsp.php, accessed on September 14, 2023) [14]. The OB and DL values were set as≥30 % and 0.18, respectively, to acquire the active compound and identify potential targets. The targets of CHB were obtained from GeneCards (https://www.genecards.org/, accessed on October 14, 2023) [15], OMIM (https://omim.org/, accessed on October 14, 2023) [16], and DisGeNET (https://www.disgenet.org/, accessed on October 14, 2023) [17]. The overlapping targets between JWYCH and CHB are shown in a Venn diagram (https://jvenn.toulouse.inrae.fr/app/example.html). The protein-protein interaction (PPI) network was constructed via STRING 12.0 (https://cn.string-db.org/, accessed on October 16, 2023) [18] and Cytoscape 3.9.1. (built-in tool Analyze Network) [19,20]. The candidate Gene Ontology (GO) and Kyoto Encyclopedia of Genes and Genomes (KEGG) terms were obtained using the ClusterProfiler R package [21], with a p-value cutoff of 0.05 and a q-value cutoff of 0.2. The structures of the small molecule ligands were downloaded from PubChem (https://pubchem.ncbi.nlm.nih.gov/), and the 3D structures of the receptor proteins were accessed from the PDB database (https://www.rcsb.org/). Autodock Tools 1.5.7 and Autodock Vina 1.1.2 were used to run the docking stimulation. Diagrams were generated using PyMOL 2.1.

2.4. Animal model and treatment

Male C57BL6/J mice (weighing 18–20g, 6–8 weeks) were obtained from Huafukang Biotechnology Co., Ltd. (Beijing, China) and housed at the scientific research center of Chengdu University of Traditional Chinese Medicine (CDUTCM). All animal-related operations were conducted in accordance with the rules set by the CDUTCM Animal Experiment Ethics Committee (Ethical No. 2022–31). Thirty mice were allocated into three groups (10 mice per group): the normal control, model, and JWYCH treatment groups.

Model and JWYCH mice were administered rAAV-HBV1.3 (1 × 10^10 GC) through hydrodynamic injection (HDI) via the tail vein [22–25]. The mice were provided a 60 % high-fat diet for 13 weeks, starting at week 10. Both groups were administered 50 mg/kg ANIT [26–28] weekly for 4 weeks. The mice in the JWYCH group were fed 6 mg/g of JWYCH for 4 consecutive weeks. After the mice were euthanized, liver and blood samples were collected.

2.5. Histologic analysis

Liver tissues were fixed in a 4 % paraformaldehyde solution, dehydrated, embedded in paraffin, and sliced for H&E staining. For Oil Red O staining, frozen sections were embedded in an optimal cutting temperature (OCT) compound and cut into thin slices. The dyeing procedure was conducted according to the instructions. Images were taken with a Sunny HS6 section scanner (Sunny, Zhejiang, China).

2.6. Serological analysis

Serum alanine aminotransferase (ALT) and aspartate aminotransferase (AST) levels were quantified using an automatic biochemical analyzer (Mindray, Shenzhen, China). The HBsAg and HBeAg levels were detected using HBsAg and HBeAg ELISA kits for mice (TW-Reagent, Shanghai, China), respectively, following the manufacturer's instructions. HBV-DNA was extracted and quantified via real-time PCR with HBV nucleic acid testing kits (Sansure, Changsha, China), following the manufacturer's guidelines.

2.7. Untargeted metabolomics analysis of mouse liver tissue

Liver tissue sample preparation: Liver tissue (100 mg) was weighed, and 1 mL of extraction solution containing 75 % methanol and chloroform (at a 9:1 ratio) and 25 % ultrapure water was added. The tissues were ground and subjected to ultrasonication for 30 min. Following centrifugation at 12,000 rpm and 4 °C for 10 min, the supernatant was collected for subsequent analysis.

Metabolomics profiling was performed at PANOMIX Biomedical Tech Co. (Suzhou, China) and the ACQUITY UPLC System (Waters, MA, USA) coupled with the Q Exactive (Thermo Fisher Scientific, USA) was utilized. The chromatography column used was an ACQUITY UPLC HSS T3 (100 × 2.1 mm, 1.8 μm) (Waters, MA, USA). The column temperature was maintained at 40 °C, with a flow rate of 0.3 mL/min and an injection volume of 2 μL. The mobile phases used for ESI (+) analysis were composed of 0.1 % formic acid in acetonitrile (B1) and 0.1 % formic acid in water (A1). For ESI (−) analysis, the mobile phases consisted of acetonitrile (B2) and 5 mM ammonium formate (A2). The washing procedure is detailed in Table 1. Both negative and positive ion modes were used for the analysis. The ESI (+) mode was 3.5 kV; the ESI (−) mode was −2.5 kV. The full scan range was *m/z* 100–1000, and the normalized collision energy was 30 eV.

Principal component analysis (PCA) and orthogonal partial least squares analysis (OPLS-DA) were conducted via MetaboAnalyst

5.0 (https://www.metaboanalyst.ca/) and SIMCA 14.1 (Umetrics AB, Västerbotten, Sweden). Metabolites with a p value < 0.05, a fold change (FC) > 2, and a variable importance in the projection (VIP) > 1 were considered potential biomarkers. MetaboAnalyst was used to perform enrichment analysis.

2.8. Combination analysis of network pharmacology and metabolomics

To investigate the interactions between gene targets and metabolites, we constructed the compound–reaction–enzyme networks using the MetScape plugin in Cytoscape [29].

2.9. Statistical analysis

Statistical analysis was performed via GraphPad Prism 9.0 (GraphPad, California, USA). The results are presented as the means ± standard deviations. The *t*-test was used to compare two groups, whereas one-way ANOVA was used to compared multiple groups. $p < 0.05$ was considered statistically significant. The minimum number of biological replications was three, and the minimum number of technical replications was one.

3. Results

3.1. Identifying the main compounds of JWYCH

UHPLC-MS/MS was utilized to examine the substances of JWYCH and identify chemical structures. The analysis was performed via Compound Discoverer 3.3. It involves determining the molecular weight, retention time, fragment ion analysis, and matching databases. The total ion chromatogram is presented in Fig. 1A and B. A total of 144 chemicals, categorized as amino acids, organic acids, flavonoids, and phenolic compounds, such as geniposide, chlorogenic acid, catechin, and gallic acid, were detected (Table S1).

3.2. Underlying mechanism of the effects of JWYCH decoction on CHB by network pharmacology analysis

A total of 48 compounds were screened out. Among them, 13, 16, 15, and 7 active compounds were identified in yinchen, dahuang, zhizi, and baizhu, respectively. After the duplicate targets were filtered, 207 putative targets were obtained. A total of 2756 disease-related targets were identified; 415 targets were extracted from DisGeNET, while 2587 targets and 145 targets were identified from GeneCards and OMIN, respectively. A total of 120 overlapping targets between the herbal prescription and the disease were identified (Fig. 2A). The main components corresponding to the common targets were quercetin, isorhamnetin, beta-sitosterol, kaempferol, and stigmasterol. The proteins were ranked by degree. The top 10 proteins were TP53, AKT1, TNF, IL6, JUN, EGFR, CASP3, HIF1A, BCL2, and IL1B (Fig. 2B).

A total of 2304 GO terms were acquired. The primary GO terms were enriched in response to oxidative stress and in response to lipopolysaccharide (Fig. 2C). Additionally, 176 KEGG terms were obtained. The main signaling pathways included the PI3K-Akt signaling pathway, the MAPK signaling pathway, and the IL-17 signaling pathway (Fig. 2D).

3.3. Molecular docking

The compounds quercetin, isorhamnetin, beta-sitosterol, kaempferol, and stigmasterol were used to bind with the target proteins TP53, AKT1, TNF, IL6, and JUN, and a heatmap (Fig. 3A) was generated to demonstrated the binding energy between the compounds and the core proteins. The binding energy of TP53 with stigmasterol was 9 kcal/mol, followed by the interaction of TP53 with beta-sitosterol. Potential binding residues included ASN-131, ASN-268, and SRE-269 (Fig. 3B and C). These findings suggest that these compounds can reduce liver damage in mice by binding to these proteins.

3.4. Effect of JWYCH on CHB mice

The ELISA results revealed that JWYCH could reduce HBeAg levels in infected the mice, while HBsAg levels and HBV-DNA copies remained unchanged relative to those in the model group (Fig. 4A–C). Additionally, the normal control group exhibited typical structures, with hepatocytes of uniform size and hepatic cords arranged radially. Within the model group, the hepatic lobules

Table 1
Gradient procedure for washing.

Time (min)	A1/A2 (%)	B1/B2 (%)
0–1	92	8
1–8	92–2	8–98
8–10	2	98
10–10.1	2–92	98–8
10.1–12	92	8

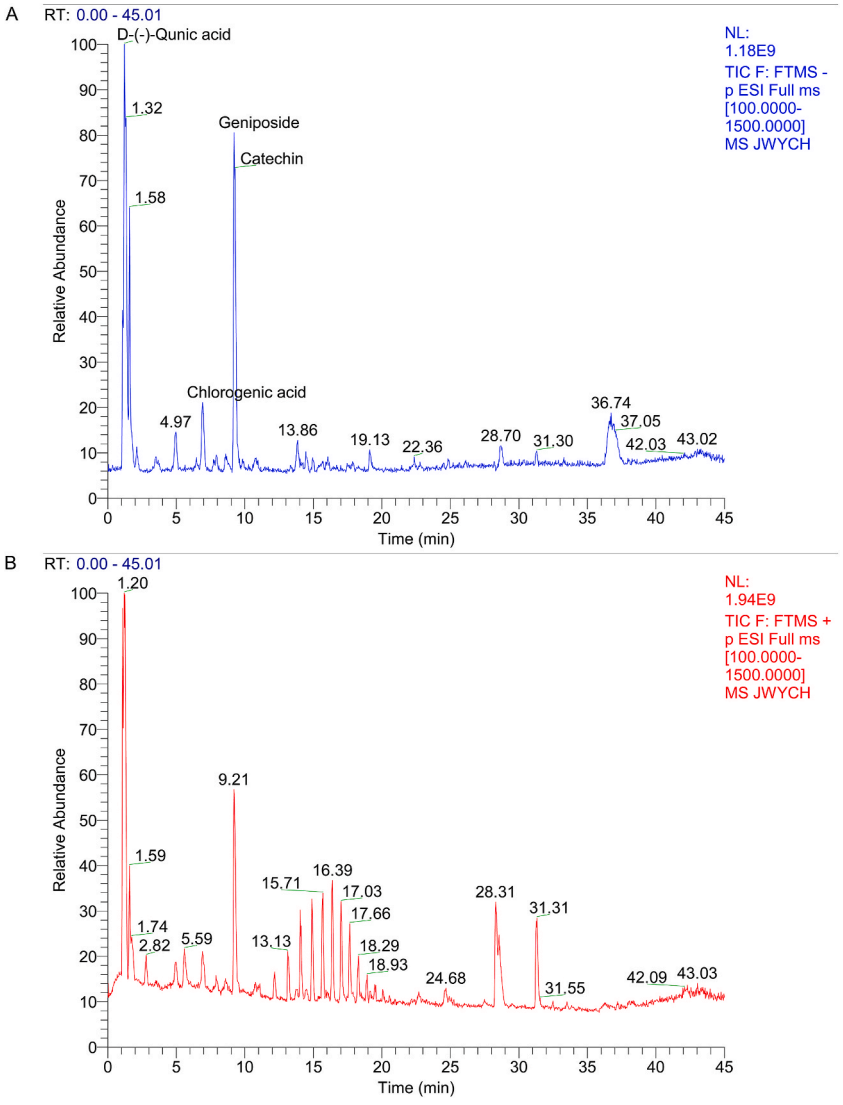

Fig. 1. Total ion chromatograms of JWYCH in negative (A) and positive (B) modes.

demonstrated disarray, whereas the liver cells exhibited looseness and swelling. Compared with the model, JWYCH improved liver function, inhibited lipid accumulation, and reduced pathological changes in the liver (Fig. 4D–F).

3.5. Metabolomics analysis

After the databases were searched and compared, 473 metabolites were identified. PCA and OPLS-DA were used to assess the metabolic alterations among the different groups (Fig. 5A–E). The separation of components indicated that the CHB model could disrupt metabolic function. Additionally, the OPLS-DA score plot clearly revealed a separation between the JWYCH and model groups, indicating that the administration of JWYCH had an effect on the metabolic profile of CHB mice. The outcome of the 200 permutations confirmed the robust and reliable prediction capability of the OPLS-DA model (Fig. 5F and G). Metabolites with VIP >1, FC > 2 or <0.5, and $p < 0.05$ were identified as potential biomarkers. The volcano plots depict the differentially abundant metabolites between the two groups (Fig. 5H and I). Furthermore, hierarchical cluster analysis was conducted to illustrate the variation characteristics, clustering, and similarity of the data (Fig. 6A and B).

Compared with those in the control group, 11 metabolites in the model group were upregulated. These included chenodeoxycholic acid, ascorbate, trans-cinnamate, sphingosine, and taurine. On the other hand, 52 metabolites such as tyramine, 8,9-EET, citric acid, retinol, and alpha-tocotrienol were downregulated.

In the comparison between the JWYCH and model groups, 21 metabolites, including pipecolic acid, alpha-terpinene, adenosine, L-phenylalanine, and L-kynurenine, were upregulated. Additionally, 84 metabolites, such as leukotriene C4, thymidine, thiamine, beta-

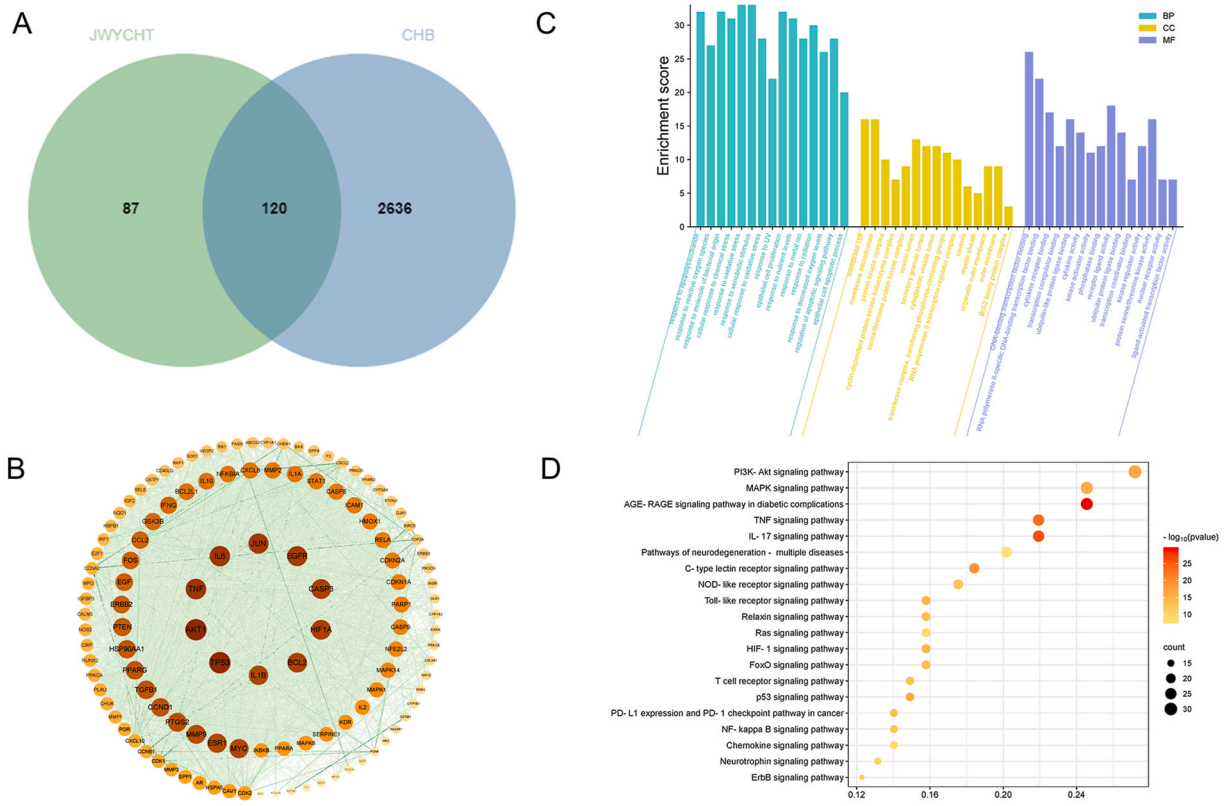

Fig. 2. Network pharmacology analysis of JWYCH for the treatment of CHB. (A) Venn diagram of JWYCH-related targets (green color) and CHB-related targets (blue color). There are 120 overlapping targets between the green and blue parts. (B) PPI network of 120 overlapping targets. Each circle represents a target; the deeper the orange color of the target node is, the greater the degree of interaction among the targets; the lines represent intersections between different targets. (C) GO analysis showing the top 20 biological process (BP), cellular component (CC), and molecular function (MF) terms. (D) KEGG analysis revealed the top 20 involved pathways. The color scale ranges from red to light gold, representing the significance of the pathways from low to high p-values; the larger the bubble is, the greater the number of targets.

tyrosine, and corticosterone, were downregulated.

3.6. Pathway analysis

MetaboAnalyst was used for KEGG analysis of the identified differentially abundant metabolites. In the control and model groups, the pathways included mainly retinol metabolism, arachidonic acid metabolism (AA) metabolism, tryptophan metabolism, taurine and hypotaurine metabolism, and primary bile acid biosynthesis (Fig. 6C).

The metabolic pathways related to JWYCH in CHB mice included phenylalanine metabolism; phenylalanine, tyrosine, and tryptophan biosynthesis; pantothenate and CoA biosynthesis; pyrimidine metabolism; arachidonic acid metabolism; and others (Fig. 6D). The effect of JWYCH was not limited to one metabolic pathway but rather involved the connection of different pathways to achieve the treatment goal.

3.7. Integrated analysis of network pharmacology and metabolomics

Differentially abundant metabolites between the JWYCH and model groups, as well as the identified targets via network analysis, were matched via the MetScape to generate networks (Fig. 7). The main pathways included retinol metabolism; arachidonic acid metabolism; tryptophan metabolism; pantothenate and CoA biosynthesis; and pyrimidine metabolism.

4. Discussion

The current therapies for CHB are unable to completely eradicate the HBV virus and carry the risk of drug resistance and adverse effects [30,31]. Currently, there are no pharmaceutical interventions capable of achieving the goal of functional curation. For an extended period, TCM has employed herbal treatments to alleviate liver diseases. Herbal compounds are being increasingly investigated for their hepatoprotective properties because of their accessibility, low toxicity, and effectiveness [32]. The efficacy of TCM

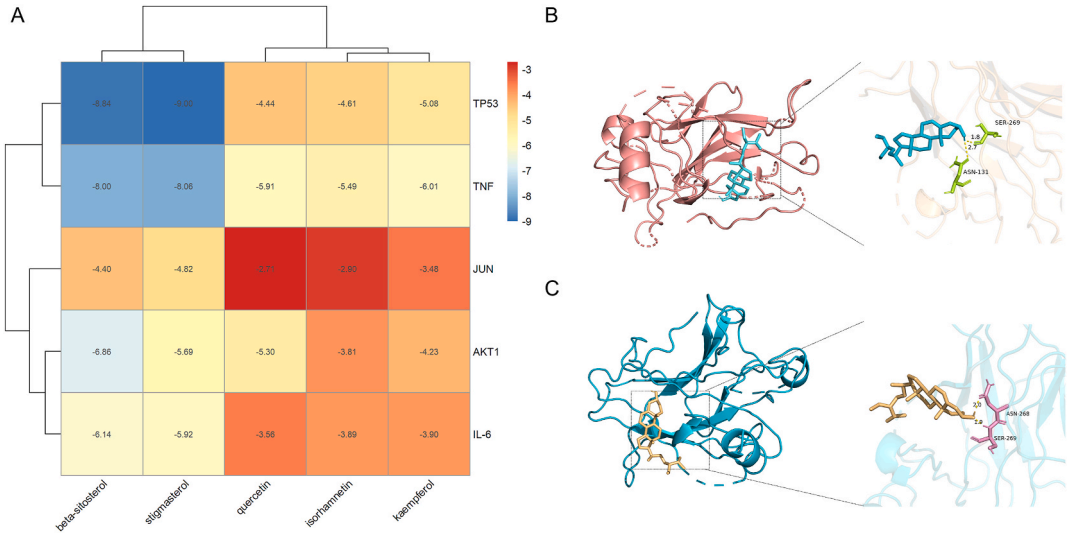

Fig. 3. Molecular docking results and representative compound–protein figures. (A) Heatmap depicting the molecular docking affinity energy scores (kcal/mol) for five compounds, beta-sitosterol, stigmasterol, quercetin, isorhamnetin, and kaempferol, docked with five proteins: TP53, TNF, JUN, AKT1, and IL-6. Lower values indicate a stronger affinity between the drug component and the protein. (B–C) Binding figures of TP53-stigmasterol and TP53-beta-sitosterol. In the enlarged figure, the yellow dotted line represents a hydrogen bond, and the number next to it indicates the distance between the two bonded components.

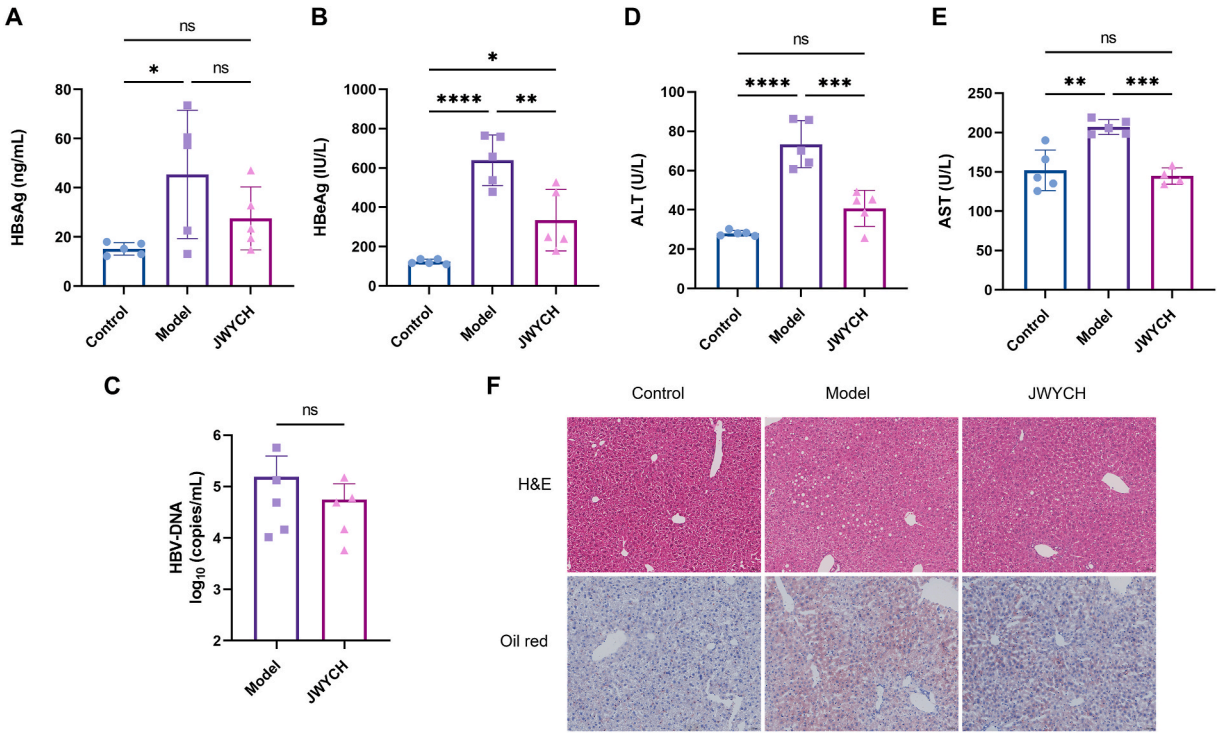

Fig. 4. Effects of JWYCH on HBV replication, liver function, and pathology in CHB mice (n = 5). (A) Serum HBsAg levels (ng/mL). (B) Serum HBeAg levels (IU/L). (C) Serum HBV-DNA $\log_{10}$ (copies/mL). (D) Serum ALT levels (U/L). (E) Serum AST levels (U/L). (F) Representative images of H&E and Oil Red O staining.Staining of mouse liver tissues (scale bar = 50 μm). Compared with the two groups, $^{*}p < 0.05$, $^{**}p < 0.01$,$^{***}p < 0.001$, $^{****}p < 0.0001$, ns: no significance.

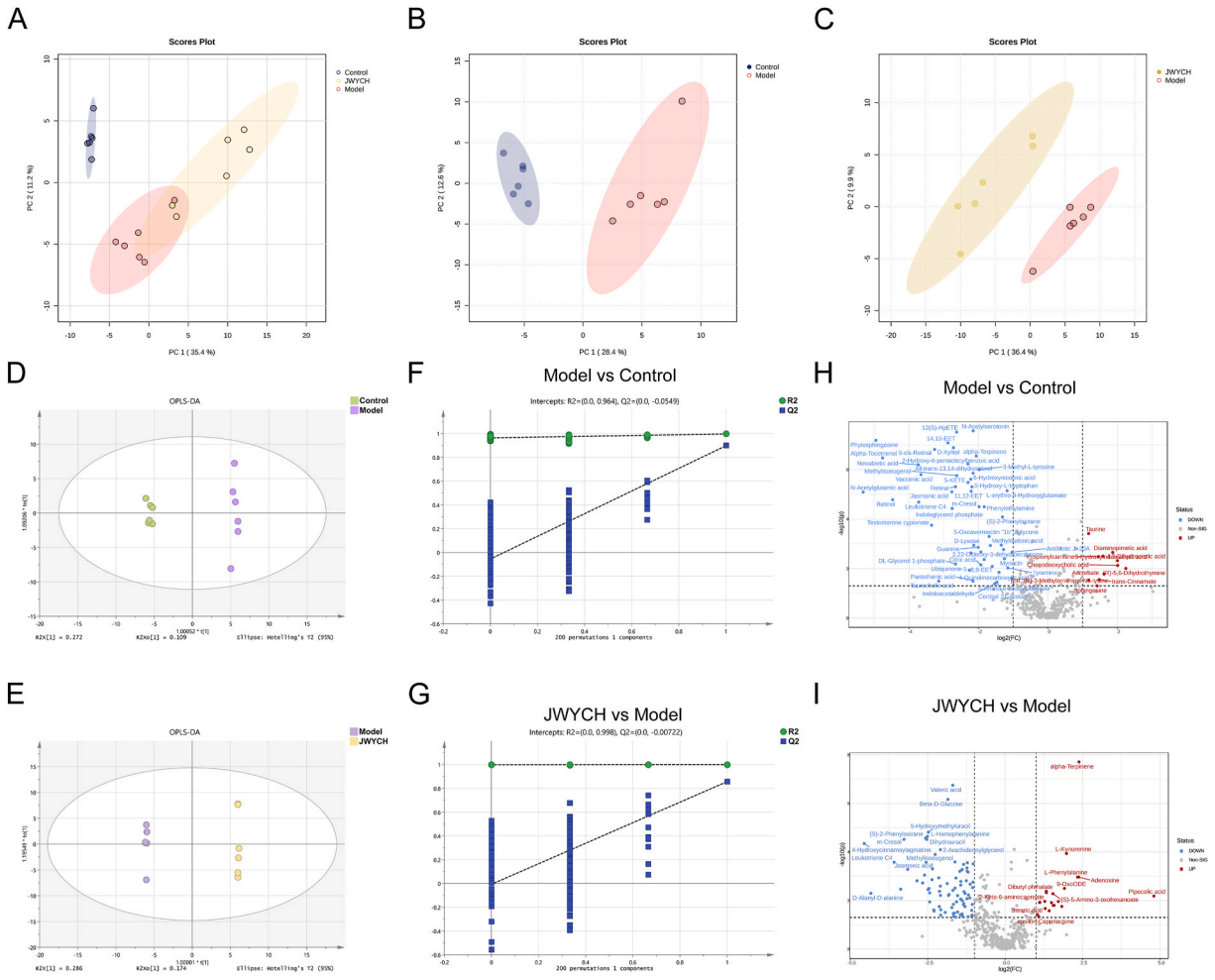

Fig. 5. Metabolomic analysis of the effects of JWYCH on CHB (n = 6). (A–C) PCA score plots of the control, model, and JWYCH groups; the control and model groups; and the model and JWYCH groups, respectively. (D–E) OPLS-DA score plots of the control and model groups and the model and JWYCH groups. (F–G) Results of 200 permutation tests for the OPLS-DA mode of the control and model groups and the model and JWYCH groups. (H–I) Volcano plots of differentially abundant metabolites analysis of the model and control groups and the JWYCH and model groups. The blue dots represent depleted metabolites, the red dots represent upregulated metabolites, and the gray dots represent metabolites that were not significantly difference between the groups.

therapy for HBV infection appears to be promising. For example, the TCM Fuzheng Huayu has been shown to reduce the occurrence of HCC in HBV-related cirrhosis patients [33]. Additionally, the classic spleen-strengthening formula Xiangsha Liujunzi decoction has the potential to improve T lymphocyte immune function in patients with decompensated hepatitis B cirrhosis [34].

The formulation JWYCH consists of YCHD and Baizhu. YCHD is a representative prescription for the treatment of CHB damp-heat syndrome and affects acute liver injury, liver steatosis, and liver fibrosis [35–37]. In accordance with TCM theory, Baizhu is believed to enhance spleen function, facilitate the flow of Qi, alleviate dampness, and facilitate diuresis. Baizhu extract has been demonstrated to be effective in the treatment of acute liver injury and the enhancement of liver function [38,39]. In this study, JWYCH treatment improved liver function, inhibited lipid deposition, alleviated liver tissue pathology, and decreased HBeAg in a mouse model. HBeAg is an indicator of HBV replication; early loss of HBeAg can reduce the risk of severe liver fibrosis and the progression of cirrhosis [40]. JWYCH showed potential as a therapeutic agent for treating CHB in a mouse model. To investigate the underlying mechanism of JWYCH in CHB, we used UHPLC-MS/MS and network pharmacology. The identified chemical markers included quercetin, catechin, and chlorogenic acid. Quercetin exhibits inhibits the replication of HBV and reduces the secretion of HBsAg and HBeAg in cell models [41]. Additionally, studies have suggested that the administration of quercetin can alleviate liver steatosis by activating AMPK activity [42]. Moreover, quercetin has been found to prevent liver carcinogenesis and may be associated with cell proliferation and apoptosis [43]. Through PPI analysis, the targets TP53, AKT1, TNF, and IL-6 were identified. TP53 is frequently studied in research related to liver diseases. The development of HCC may be connected to the TP53 mutation. Studies indicate that HBV-related liver tumors exhibit a greater frequency of TP53-inactivating mutations than non-HBV-related liver tumors do [44,45]. When liver damage occurs, macrophages play a crucial role in the inflammatory response, and are the primary cells that release various inflammatory mediators,

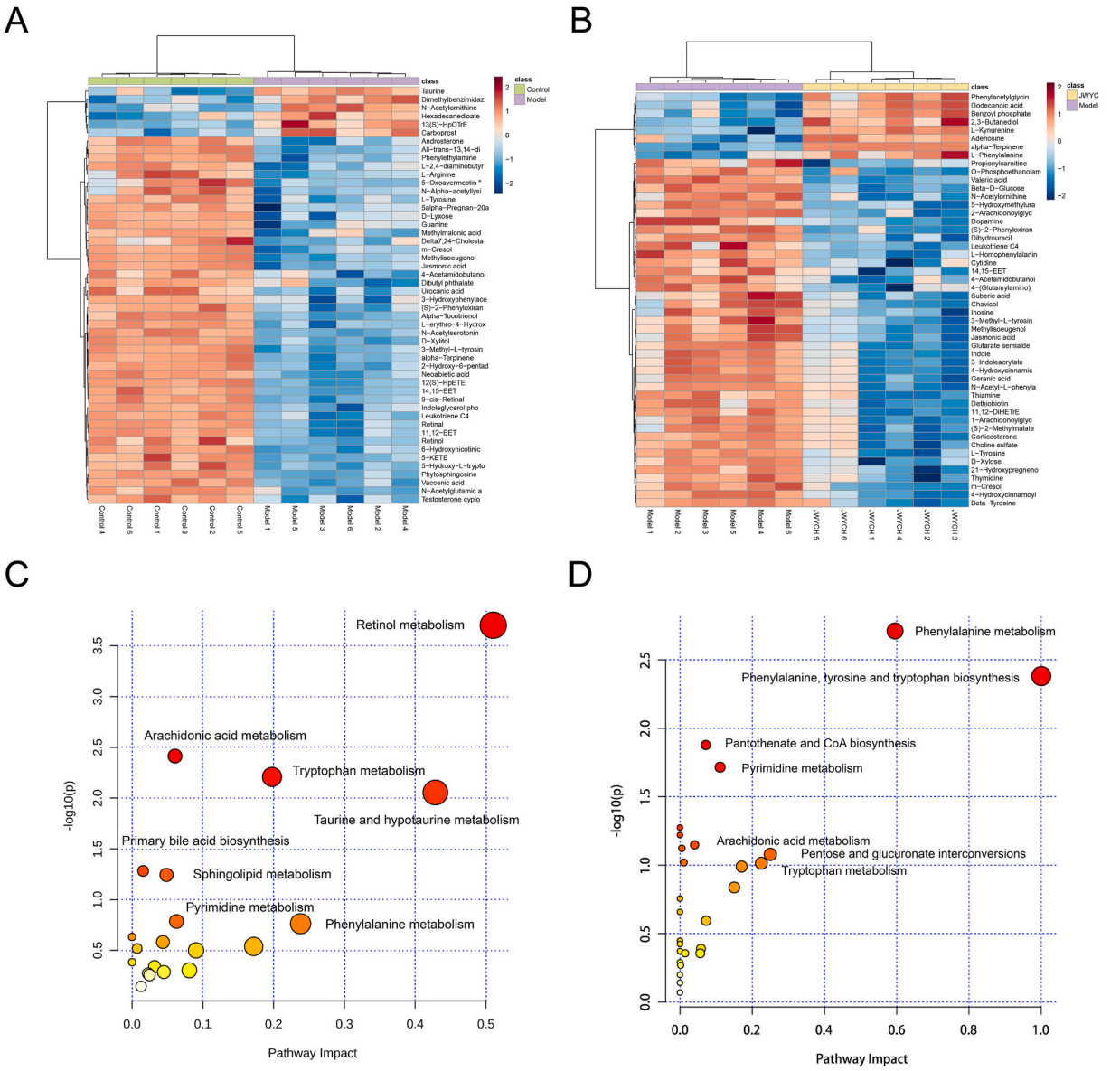

Fig. 6. (A–B) Hierarchical cluster analysis heatmap showing the relative abundance of differentially abundant metabolites in the control group vs. model group, as well as the model group vs. JWYCH group. The color scale ranges from red to blue, representing high to low relative abundance. (C–D) Metabolic pathway enrichment analysis of differentially abundant metabolites between the control and model groups and between the model and JWYCH groups. The redder the dot color is, the smaller the p-value; the larger the dot size is, the greater the pathway impact.

such as IL-6 [46]. The enriched pathways, such as the MAPK, AGE-RAGE, IL-17, and TNF signaling pathways, are related to the inflammatory response and immune regulation. In the AGE-RAGE pathway, AGEs can crosslink with collagen and elastin and increase tissue stiffness [47]. When AGEs interact with RAGE, NADPH-oxidase is activated by the production of ROS, and activated NF-κB triggers the activation of IL-6 and TNF-α [48]. IL-17 can lead to MAPK and NF-κB pathway activation, exacerbate inflammation, and cause hepatocyte damage [49].

Metabolites serve as substrates for metabolic activities and as signal molecules for cellular processes [50]. Many altered metabolites were identified in the CHB mouse model in this study; for example, alpha-tocotrienol was decreased, whereas ascorbate was increased, suggesting that the CHB mouse model is linked to oxidative stress. In addition, amino acid-derived metabolites such as 4,5-dihydroorotic acid, propionylcarnitine, and taurine were increased, suggesting that the catabolism of amino acids was accelerated in the CHB mouse model. Moreover, the level of chenodeoxycholic acid (CDCA), a primary bile acid (BA), increased in the CHB mouse model but was reversed with JWYCH treatment. BA synthesis occurs in the liver, and the alternative pathway is initiated by CYP27A1, which is further hydroxylated by CYP7B1 [51]. Infants with a genetic deficiency in CYP7B1 rapidly progress from hepatic inflammation to severe fibrosis [52]. Recent research has also indicated that altered metabolite production in bile acid metabolism is linked to HBV

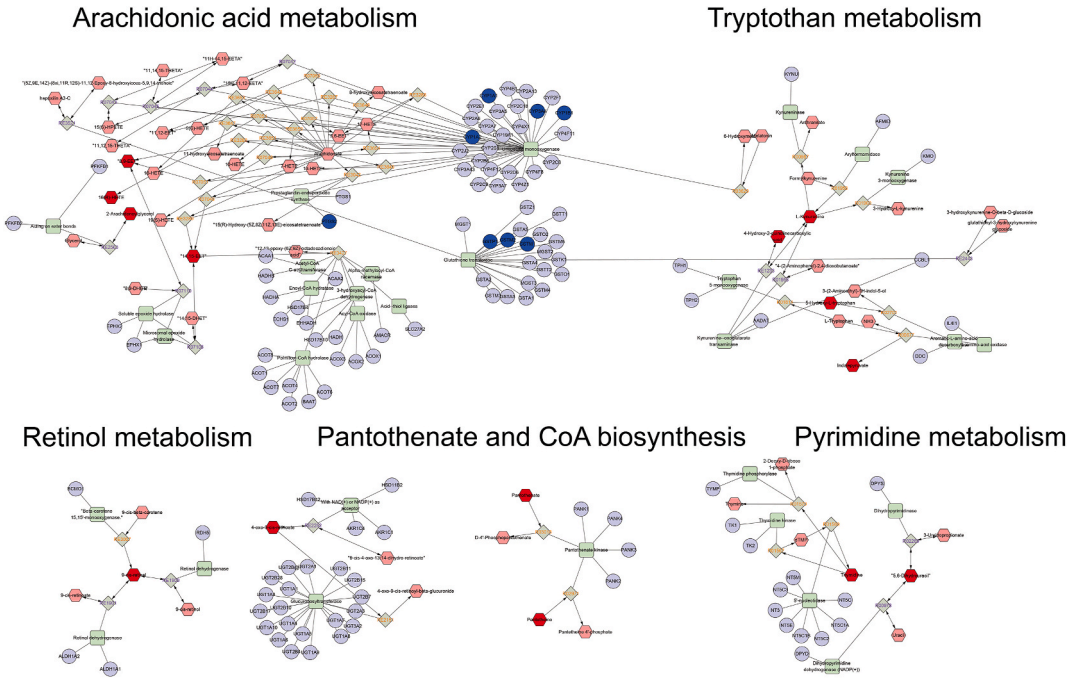

Fig. 7. Compound–reaction–enzyme–gene networks of the key metabolites between the model groups and the JWYCH group. The blue ellipses are the input key genes, and the red hexagons are the input key metabolites. The rose-red hexagons, lavender ellipses, light cyan round rectangles, and light gray diamonds represent active compounds, genes, enzymes, and reactions, respectively.

infection, liver fibrosis, and cirrhosis [53,54]. Moreover, BAs exert immunomodulatory effects through the release of cytokines from hepatocytes and immune cells [55]. BAs can also influence the MAPK pathway and activate p53, NF-κB, and the JAK-STAT3 pathway, leading to inflammation and HCC progression [56]. BAs promote the production of arachidonic acid (AA) metabolites by activating epidermal growth factor, leading to the upregulation of cyclooxygenase and lipoxygenase. AA is a prominent lipid component that serves as the main source of free fatty acids (FFAs) generated by phospholipase A2 (PLA2). It has pro-inflammatory properties with significant biological implications [57]. The metabolites derived from AA involved in the regulation of liver and gallbladder physiological functions can cause the release of oxygen-free radicals and lysosomal enzymes, as well as increase vascular permeability. Additionally, hepatitis B virus X (HBx) protein can release AA metabolites to activate ERK1/2, promoting HCC proliferation [58]. In this study, the AA metabolites 8,9-EET, 14,15-EET, 16(R)-HETE, and prostaglandin-c2 were decreased in mice treated with JWYCH, indicating that JWCYH affects AA metabolism.

JWYCH also participates in regulating amino acid metabolism. In the JWYCH group, L-phenylalanine increased, whereas L-tyrosine and beta-tyrosine decreased. These amino acids are classified as aromatic amino acids and play crucial roles in protein synthesis. Elevated phenylalanine levels not only affect metabolism but also interfere with T-cell activation, compromising the immune response of the human body [59,60]. In this study, 5-hydroxy-L-tryptophan decreased in the model group but was restored in the JWYCH group. Tryptophan metabolism changes could affect alterations in the kynurenic acid pathway, which contributes to the regulation of the inflammatory process. Moreover, it can act as an N-methyl-D-aspartic acid receptor antagonist and reduce IFN-γ secretion [61], whereas IFN-γ is related to the anti-HBV immune response. Moreover, retinol metabolism is involved in JWCYH therapy. The metabolite retinoic acid (RA) is stored in the lipid droplets of hepatic stellate cells (HSCs) and regulates regulatory T cell exhaustion in hepatitis [62–64]. However, RA may inhibit T cell responses and delay viral clearance; thus, combining antiviral therapy with RA could help prevent fulminant viral hepatitis [65].

Therefore, we hypothesized that JWYCH treatment of CHB is associated with oxidative stress and immune response processes, which are jointly mediated through the metabolism of bile acid, arachidonic acid, retinol, and other metabolic pathways. The differentially abundant metabolites identified in this study may serve as potential biomarkers for CHB. The study of the JWYCH mechanism will provide new perspectives for the treatment of CHB.

Several limitations require discussion; the ingredients of JWYCH are complex, and the predictions from bioinformatics require more experimental validation. In future studies, we will further investigate the exact mechanisms of JWYCH in CHB and conduct targeted metabolomics and clinical studies to confirm these findings.

5. Conclusion

In conclusion, JWYCH could reduce the serum ALT, AST, and HBeAg levels and ameliorate liver injuries and lipid droplets in CHB mice. The effect of JWYCH is likely associated with regulating the metabolism of bile acid, arachidonic acid, and retinol. These

differentially abundant metabolites may serve as potential biomarkers for CHB, and JWYCH may provide new perspectives for the treatment of CHB.

Ethics statement

All animal experiments were approved by the Chengdu University of Traditional Chinese Medicine Animal Experiment Ethics Committee (Ethical No: 2022–31)

Data availability statement

Data will be made available on request.

CRediT authorship contribution statement

Xinyi Xu: Writing – original draft, Investigation, Formal analysis. **Jin Liu:** Visualization, Methodology, Investigation. **Xue Li:** Visualization, Methodology, Investigation. **QuanSheng Feng:** Supervision. **Yue Su:** Writing – review & editing, Supervision, Funding acquisition.

Declaration of competing interest

The authors declare that they have no known competing financial interests or personal relationships that could have appeared to influence the work reported in this paper.

Acknowledgments

The study was supported by the National Natural Science Foundation of China (Grant No. 82204956), the Science and Technology Department of Sichuan Province (Grant No. 2022YFS0409), the College of Basic Medical Sciences 2022 Legacy Innovation Fund (CCCXYB202207), and the Chengdu University of Traditional Chinese Medicine 2024 Joint University-Institute Innovation Fund (LHJJ202402016).

Appendix A. Supplementary data

Supplementary data to this article can be found online at https://doi.org/10.1016/j.heliyon.2024.e36267.

References

[1] W.H.O. (WHO), Hepatitis B. https://www.who.int/en/news-room/fact-sheets/detail/hepatitis-b, 2024. (Accessed 14 June 2024).
[2] P. Revill, B. Testoni, S. Locarnini, F. Zoulim, Global strategies are required to cure and eliminate HBV infection, Nat. Rev. Gastroenterol. Hepatol. 13 (4) (2016) 239–248.
[3] H. Kwon, A.S. Lok, Hepatitis B therapy, Nat. Rev. Gastroenterol. Hepatol. 8 (5) (2011) 275–284.
[4] M. Deng, H.J. Chen, J.Y. Long, J.W. Song, L. Xie, X.F. Li, Atractylenolides (I, II, and III): a review of their pharmacology and pharmacokinetics, Arch Pharm. Res. (Seoul) 44 (7) (2021) 633–654.
[5] S. Song, J. Zheng, D. Zhao, A. Zheng, Y. Zhu, Q. Xu, T. Liu, Quantitative proteomics analysis based on data-independent acquisition reveals the effect of Shenling Baizhu powder (SLP) on protein expression in MAFLD rat liver tissue, Clin. Proteonomics 20 (1) (2023) 55.
[6] Z. Yao, J. Guo, B. Du, L. Hong, Y. Zhu, X. Feng, Y. Hou, A. Shi, Effects of Shenling Baizhu powder on intestinal microflora metabolites and liver mitochondrial energy metabolism in nonalcoholic fatty liver mice, Front. Microbiol. 14 (2023) 1147067.
[7] J.Y. Li, H.Y. Cao, L. Sun, R.F. Sun, C. Wu, Y.Q. Bian, S. Dong, P. Liu, M.Y. Sun, Therapeutic mechanism of Yin-Chen-Hao decoction in hepatic diseases, World J. Gastroenterol. 23 (7) (2017) 1125–1138.
[8] Y.L. Wu, Z.L. Li, X.B. Zhang, H. Liu, Yinchenhao decoction attenuates obstructive jaundice-induced liver injury and hepatocyte apoptosis by suppressing protein kinase RNA-like endoplasmic reticulum kinase-induced pathway, World J. Gastroenterol. 25 (41) (2019) 6205–6221.
[9] G.C. Song, B. Zou, J. Zhao, F.Y. Weng, Y. Li, X.Q. Xu, S. Zhang, D.M. Yan, J.Y. Jin, X. Sun, C.H. Liu, F.R. Qiu, Yinchen decoction protects against cholic acid diet-induced cholestatic liver injury in mice through liver and ileal FXR signaling, J. Ethnopharmacol. 313 (2023).
[10] J. Lucifora, A. Salvetti, X. Marniquet, L. Mailly, B. Testoni, F. Fusil, A. Inchauspe, M. Michelet, M.L. Michel, M. Levrero, P. Cortez, T.F. Baumert, F.L. Cosset, C. Challier, F. Zoulim, D. Durantel, Detection of the hepatitis B virus (HBV) covalently-closed-circular DNA (cccDNA) in mice transduced with a recombinant AAV-HBV vector, Antivir. Res. 145 (2017) 14–19.
[11] Y. Teng, Z.C. Xu, K.T. Zhao, Y.Q. Zhong, J.J. Wang, L. Zhao, Z.X. Zheng, W. Hou, C.L. Zhu, X.W. Chen, U. Protzer, Y. Li, Y.C. Xia, Novel function of SART1 in HNF4α transcriptional regulation contributes to its antiviral role during HBV infection, J. Hepatol. 75 (5) (2021) 1072–1082.
[12] L. Chen, W.Y. Lu, L. Wang, X. Xing, Z.Y. Chen, X. Teng, X.F. Zeng, A.D. Muscarella, Y.H. Shen, A. Cowan, M.R. McReynolds, B.J. Kennedy, A.M. Lato, S. R. Campagna, M. Singh, J.D. Rabinowitz, Metabolite discovery through global annotation of untargeted metabolomics data, Nat. Methods 18 (11) (2021) 1377–+.
[13] C.H. Johnson, J. Ivanisevic, G. Siuzdak, Metabolomics: beyond biomarkers and towards mechanisms, Nat. Rev. Mol. Cell Biol. 17 (7) (2016) 451–459.
[14] J. Ru, P. Li, J. Wang, W. Zhou, B. Li, C. Huang, P. Li, Z. Guo, W. Tao, Y. Yang, X. Xu, Y. Li, Y. Wang, L. Yang, TCMSP: a database of systems pharmacology for drug discovery from herbal medicines, J. Cheminf. 6 (2014) 13.
[15] M. Safran, I. Dalah, J. Alexander, N. Rosen, T. Iny Stein, M. Shmoish, N. Nativ, I. Bahir, T. Doniger, H. Krug, A. Sirota-Madi, T. Olender, Y. Golan, G. Stelzer, A. Harel, D. Lancet, GeneCards Version 3: the human gene integrator, Database 2010 (2010) baq020.

[16] A. Hamosh, J.S. Amberger, C. Bocchini, A.F. Scott, S.A. Rasmussen, Online mendelian inheritance in man (OMIM(R)): victor McKusick's magnum opus, Am. J. Med. Genet. 185 (11) (2021) 3259–3265.
[17] J. Pinero, A. Bravo, N. Queralt-Rosinach, A. Gutierrez-Sacristan, J. Deu-Pons, E. Centeno, J. Garcia-Garcia, F. Sanz, L.I. Furlong, DisGeNET: a comprehensive platform integrating information on human disease-associated genes and variants, Nucleic Acids Res. 45 (D1) (2017) D833–D839.
[18] D. Szklarczyk, R. Kirsch, M. Koutrouli, K. Nastou, F. Mehryary, R. Hachilif, A.L. Gable, T. Fang, N.T. Doncheva, S. Pyysalo, P. Bork, L.J. Jensen, C. von Mering, The STRING database in 2023: protein-protein association networks and functional enrichment analyses for any sequenced genome of interest, Nucleic Acids Res. 51 (D1) (2023) D638–D646.
[19] M. Franz, C.T. Lopes, D. Fong, M. Kucera, M. Cheung, M.C. Siper, G. Huck, Y. Dong, O. Sumer, G.D. Bader, Cytoscape.js 2023 update: a graph theory library for visualization and analysis, Bioinformatics 39 (1) (2023).
[20] P. Shannon, A. Markiel, O. Ozier, N.S. Baliga, J.T. Wang, D. Ramage, N. Amin, B. Schwikowski, T. Ideker, Cytoscape: a software environment for integrated models of biomolecular interaction networks, Genome Res. 13 (11) (2003) 2498–2504.
[21] T. Wu, E. Hu, S. Xu, M. Chen, P. Guo, Z. Dai, T. Feng, L. Zhou, W. Tang, L. Zhan, X. Fu, S. Liu, X. Bo, G. Yu, clusterProfiler 4.0: a universal enrichment tool for interpreting omics data, Innovation 2 (3) (2021) 100141.
[22] Y.A. Bu, K.T. Zhao, Z.C. Xu, Y.C. Zheng, R. Hua, C.J. Wu, C.L. Zhu, Y.C. Xia, X.M. Cheng, Antibiotic-induced gut bacteria depletion has no effect on HBV replication in HBV immune tolerance mouse model, Virol. Sin. 38 (3) (2023) 335–343.
[23] D. Yang, L. Liu, D. Zhu, H. Peng, L. Su, Y.X. Fu, L. Zhang, A mouse model for HBV immunotolerance and immunotherapy, Cell. Mol. Immunol. 11 (1) (2014) 71–78.
[24] C. Ko, J. Su, J. Festag, R. Bester, A.D. Kosinska, U. Protzer, Intramolecular recombination enables the formation of hepatitis B virus (HBV) cccDNA in mice after HBV genome transfer using recombinant AAV vectors, Antivir. Res. 194 (2021) 105140.
[25] Y. Teng, Z. Xu, K. Zhao, Y. Zhong, J. Wang, L. Zhao, Z. Zheng, W. Hou, C. Zhu, X. Chen, U. Protzer, Y. Li, Y. Xia, Novel function of SART1 in HNF4alpha transcriptional regulation contributes to its antiviral role during HBV infection, J. Hepatol. 75 (5) (2021) 1072–1082.
[26] X. Lv, Y. Liu, S. Liu, Y. Liu, Y. Qu, Q. Cai, Metabonomics and pharmacodynamics studies of Gentiana radix and wine-processed Gentiana radix in damp-heat jaundice syndrome rats, J. Ethnopharmacol. 332 (2024) 118291.
[27] H. Su, Q. Wang, Y. Li, J. Jin, B. Tan, D. Yan, B. Zou, G. Song, F. Weng, F. Qiu, Effect of different ratios of yinchen and gancao decoction on ANIT-treated cholestatic liver injury in mice and its potential underlying mechanism, Front. Pharmacol. 12 (2021) 611610.
[28] D. Hu, H. Wang, H. Wang, Y. Wang, X. Wan, W. Yan, X. Luo, Q. Ning, Non-alcoholic hepatic steatosis attenuates hepatitis B virus replication in an HBV-immunocompetent mouse model, Hepatol Int 12 (5) (2018) 438–446.
[29] A. Karnovsky, T. Weymouth, T. Hull, V.G. Tarcea, G. Scardoni, C. Laudanna, M.A. Sartor, K.A. Stringer, H.V. Jagadish, C. Burant, B. Athey, G.S. Omenn, Metscape 2 bioinformatics tool for the analysis and visualization of metabolomics and gene expression data, Bioinformatics 28 (3) (2012) 373–380.
[30] C.L. Lai, D.K. Wong, G.T. Wong, W.K. Seto, J. Fung, M.F. Yuen, Rebound of HBV DNA after cessation of nucleos/tide analogues in chronic hepatitis B patients with undetectable covalently closed, JHEP Rep 2 (3) (2020) 100112.
[31] D. Durantel, F. Zoulim, New antiviral targets for innovative treatment concepts for hepatitis B virus and hepatitis delta virus, J. Hepatol. 64 (1 Suppl) (2016) S117–S131.
[32] Y. Zhou, J. Wang, D. Zhang, J. Liu, Q. Wu, J. Chen, P. Tan, B. Xing, Y. Han, P. Zhang, X. Xiao, J. Pei, Mechanism of drug-induced liver injury and hepatoprotective effects of natural drugs, Chin. Med. 16 (1) (2021) 135.
[33] H. Fan, S. Lei, Z. Zhao, Y. Huang, H. Wang, X. Liu, X. Li, M. Xu, W. Zhang, K. Sun, H. Xing, Y. Mei, J. Huang, C. Zhu, K. Zhang, Y. Zong, X. Shen, Q. Xie, C. Liu, Beneficial effects of traditional Chinese medicine Fuzheng Huayu on the occurrence of hepatocellular carcinoma in patients with compensated chronic hepatitis B cirrhosis receiving entecavir: a multicenter retrospective cohort study, J Clin Transl Hepatol 12 (5) (2024) 505–515.
[34] Y. Li, L. Ren, H. Xu, J. Liu, H. Li, F. Zhu, Effect of Xiangsha Liujunzi Decoction combined with Entecavir on T cell subsets in patients with decompensation period of hepatitis B cirrhosis, Chin J Integr Tradit West Med Dig 32 (1) (2024) 35–41.
[35] H. Cai, Y.H. Song, W.J. Xia, M.W. Jin, Aqueous extract of Yin-Chen-Hao decoction, a traditional Chinese prescription, exerts protective effects on concanavalin A-induced hepatitis in mice through inhibition of NF-kappaB, J. Pharm. Pharmacol. 58 (5) (2006) 677–684.
[36] S.D. Chen, Y. Fan, W.J. Xu, Effects of yinchenhao decoction (see text) for non-alcoholic steatohepatitis in rats and study of the mechanism, J. Tradit. Chin. Med. 31 (3) (2011) 220–223.
[37] C. Liu, M. Sun, X. Yan, L. Han, Y. Zhang, C. Liu, H. El-Nezami, P. Liu, Inhibition of hepatic stellate cell activation following Yinchenhao decoction administration to dimethylnitrosamine-treated rats, Hepatol. Res. 38 (9) (2008) 919–929.
[38] B. Han, Y. Gao, Y.L. Wang, L. Wang, Z.H. Shang, S. Wang, J. Pei, Protective effect of a polysaccharide from Macrocephalae on acute liver injury in mice, Int. J. Biol. Macromol. 87 (2016) 85–91.
[39] A.M. Wang, Z.M. Xiao, L.P. Zhou, J. Zhang, X.M. Li, Q.C. He, The protective effect of atractylenolide I on systemic inflammation in the mouse model of sepsis created by cecal ligation and puncture, Pharm. Biol. 54 (1) (2016) 146–150.
[40] Y.F. Liaw, J.J. Sung, W.C. Chow, G. Farrell, C.Z. Lee, H. Yuen, T. Tanwandee, Q.M. Tao, K. Shue, O.N. Keene, J.S. Dixon, D.F. Gray, J. Sabbat, G. Cirrhosis Asian Lamivudine Multicentre Study, Lamivudine for patients with chronic hepatitis B and advanced liver disease, N. Engl. J. Med. 351 (15) (2004) 1521–1531.
[41] Z.K. Cheng, G. Sun, W. Guo, Y.Y. Huang, W.H. Sun, F. Zhao, K.H. Hu, Inhibition of hepatitis B virus replication by quercetin in human hepatoma cell lines, Virol. Sin. 30 (4) (2015) 261–268.
[42] H. Zeng, X. Guo, F. Zhou, L. Xiao, J. Liu, C. Jiang, M. Xing, P. Yao, Quercetin alleviates ethanol-induced liver steatosis associated with improvement of lipophagy, Food Chem. Toxicol. 125 (2019) 21–28.
[43] M.L. Casella, J.P. Parody, M.P. Ceballos, A.D. Quiroga, M.T. Ronco, D.E. Frances, J.A. Monti, G.B. Pisani, C.E. Carnovale, M.C. Carrillo, M. de Lujan Alvarez, Quercetin prevents liver carcinogenesis by inducing cell cycle arrest, decreasing cell proliferation and enhancing apoptosis, Mol. Nutr. Food Res. 58 (2) (2014) 289–300.
[44] A. Takai, H.T. Dang, X.W. Wang, Identification of drivers from cancer genome diversity in hepatocellular carcinoma, Int. J. Mol. Sci. 15 (6) (2014) 11142–11160.
[45] L.N. Qi, T. Bai, Z.S. Chen, F.X. Wu, Y.Y. Chen, B.D. Xiang, T. Peng, Z.G. Han, L.Q. Li, The p53 mutation spectrum in hepatocellular carcinoma from Guangxi, China : role of chronic hepatitis B virus infection and aflatoxin B1 exposure, Liver Int. 35 (3) (2015) 999–1009.
[46] H.R. Hu, X.Y. Cheng, F. Li, Z. Guan, J. Xu, D.M. Wu, Y.Y. Gao, X.Y. Zhan, P. Wang, H.M. Zhou, Z.Q. Rao, F. Cheng, Defective efferocytosis by aged macrophages promotes STING signaling mediated inflammatory liver injury, Cell Death Dis. 9 (1) (2023).
[47] D.R. Sell, V.M. Monnier, Molecular basis of arterial stiffening: role of glycation - a mini-review, Gerontology 58 (3) (2012) 227–237.
[48] K. Prasad, AGE-RAGE stress play a role in aortic aneurysm: a comprehensive review and novel potential therapeutic target, Rev. Cardiovasc. Med. 20 (4) (2019) 201–208.
[49] S. Luo, M. Huang, X. Lu, M. Zhang, H. Xiong, X. Tan, X. Deng, W. Zhang, X. Ma, J. Zeng, T. Efferth, Optimized therapeutic potential of Yinchenhao decoction for cholestatic hepatitis by combined network meta-analysis and network pharmacology, Phytomedicine 129 (2024) 155573.
[50] Y.P. Wang, J.T. Li, J. Qu, M. Yin, Q.Y. Lei, Metabolite sensing and signaling in cancer, J. Biol. Chem. 295 (33) (2020) 11938–11946.
[51] A. Wahlstrom, S.I. Sayin, H.U. Marschall, F. Backhed, Intestinal crosstalk between bile acids and microbiota and its impact on host metabolism, Cell Metabol. 24 (1) (2016) 41–50.
[52] D. Dai, P.B. Mills, E. Footitt, P. Gissen, P. McClean, J. Stahlschmidt, I. Coupry, J. Lavie, F. Mochel, C. Goizet, T. Mizuochi, A. Kimura, H. Nittono, K. Schwarz, P. J. Crick, Y. Wang, W.J. Griffiths, P.T. Clayton, Liver disease in infancy caused by oxysterol 7 alpha-hydroxylase deficiency: successful treatment with chenodeoxycholic acid, J. Inherit. Metab. Dis. 37 (5) (2014) 851–861.
[53] G.X. Xie, R.Q. Jiang, X.N. Wang, P. Liu, A.H. Zhao, Y.R. Wu, F.J. Huang, Z.P. Liu, C. Rajani, X.J. Zheng, J.N. Qiu, X.L. Zhang, S.W. Zhao, H. Bian, X. Gao, B. C. Sun, W. Jia, Conjugated secondary 12α-hydroxylated bile acids promote liver fibrogenesis, EBioMedicine 66 (2021).

[54] X.N. Wang, G.X. Xie, A.H. Zhao, X.J. Zheng, F.J. Huang, Y.X. Wang, C. Yao, W. Jia, P. Liu, Serum bile acids are associated with pathological progression of hepatitis B-induced cirrhosis, J. Proteome Res. 15 (4) (2016) 1126–1134.
[55] C.D. Fuchs, M. Trauner, Role of bile acids and their receptors in gastrointestinal and hepatic pathophysiology, Nat. Rev. Gastroenterol. Hepatol. 19 (7) (2022) 432–450.
[56] W. Jia, G. Xie, W. Jia, Bile acid-microbiota crosstalk in gastrointestinal inflammation and carcinogenesis, Nat. Rev. Gastroenterol. Hepatol. 15 (2) (2018) 111–128.
[57] S. Chauhan, U. Devi, V.R. Kumar, V. Kumar, F. Anwar, G. Kaithwas, Dual inhibition of arachidonic acid pathway by mulberry leaf extract, Inflammopharmacology 23 (1) (2015) 65–70.
[58] C. Shan, F. Xu, S. Zhang, J. You, X. You, L. Qiu, J. Zheng, L. Ye, X. Zhang, Hepatitis B virus X protein promotes liver cell proliferation via a positive cascade loop involving arachidonic acid metabolism and p-ERK1/2, Cell Res. 20 (5) (2010) 563–575.
[59] B. Yang, X. Wang, X. Ren, Amino acid metabolism related to immune tolerance by MDSCs, Int. Rev. Immunol. 31 (3) (2012) 177–183.
[60] C.Y. Chen, C. Crowther, M.C. Kew, A. Kramvis, A valine to phenylalanine mutation in the precore region of hepatitis B virus causes intracellular retention and impaired secretion of HBe-antigen, Hepatol. Res. 38 (6) (2008) 580–592.
[61] J. Kindler, C.K. Lim, C.S. Weickert, D. Boerrigter, C. Galletly, D. Liu, K.R. Jacobs, R. Balzan, J. Bruggemann, M. O'Donnell, R. Lenroot, G.J. Guillemin, T. W. Weickert, Dysregulation of kynurenine metabolism is related to proinflammatory cytokines, attention, and prefrontal cortex volume in schizophrenia, Mol. Psychiatr. 25 (11) (2020) 2860–2872.
[62] L. Lu, Q. Lan, Z. Li, X. Zhou, J. Gu, Q. Li, J. Wang, M. Chen, Y. Liu, Y. Shen, D.D. Brand, B. Ryffel, D.A. Horwitz, F.P. Quismorio, Z. Liu, B. Li, N.J. Olsen, S. G. Zheng, Critical role of all-trans retinoic acid in stabilizing human natural regulatory T cells under inflammatory conditions, Proc Natl Acad Sci U S A 111 (33) (2014) E3432–E3440.
[63] S. Ichikawa, D. Mucida, A.J. Tyznik, M. Kronenberg, H. Cheroutre, Hepatic stellate cells function as regulatory bystanders, J. Immunol. 186 (10) (2011) 5549–5555.
[64] A. Geerts, History, heterogeneity, developmental biology, and functions of quiescent hepatic stellate cells, Semin. Liver Dis. 21 (3) (2001) 311–335.
[65] Z. Jie, Y. Liang, P. Yi, H. Tang, L. Soong, Y. Cong, K. Zhang, J. Sun, Retinoic acid regulates immune responses by promoting IL-22 and modulating S100 proteins in viral hepatitis, J. Immunol. 198 (9) (2017) 3448–3460.